

Selectivity of the complexation reactions of four regioisomeric methylcamphorquinoxaline ligands with gold(III): X-ray, NMR and DFT investigations



Biljana Đ. Glišić^{a,b}, Marcin Hoffmann^b, Beata Warżajtis^b, Marija S. Genčić^c, Polina D. Blagojević^c, Niko S. Radulović^{c,*}, Urszula Rychlewska^{b,*}, Miloš I. Djuran^{a,*}

^a Department of Chemistry, Faculty of Science, University of Kragujevac, R. Domanovića 12, 34000 Kragujevac, Serbia

^b Faculty of Chemistry, Adam Mickiewicz University, Umultowska 89B, 61-614 Poznań, Poland

^c Department of Chemistry, Faculty of Science and Mathematics, University of Niš, Višegradska 33, 18000 Niš, Serbia

ARTICLE INFO

Article history:

Received 12 November 2015

Accepted 7 December 2015

Available online 15 December 2015

Keywords:

Gold(III)

Camphorquinoxaline

NMR spectroscopy

X-ray crystallography

DFT calculations

ABSTRACT

Reported are the synthesis, spectral and structural characteristics of new quinoxaline-related regioisomeric ligands **L1–L4** (1, x, 11, 11-tetramethyl-1,2,3,4-tetrahydro-1,4-methanophenazine, x = 7, 8, 9 and 6, respectively) and their mononuclear Au(III) complexes (**1–4**). Fusion of the camphor moiety to the quinoxaline core made two N-atoms of quinoxaline nonequivalent while the introduction of a methyl-substituent at positions 6–9 enabled a tuning of coordination properties of **L1–L4**. Gold(III) complexes **1–4** and ligands **L1–L4** have been studied in detailed by 1D and 2D NMR and the structures of **1–4** have been determined by X-ray crystallography. The results of these analyses revealed a regiospecific coordination of Au(III) to the sterically less hindered N-5 atom (spatially close to the non-substituted bridgehead carbon) of **L1–L3**, and to N-10 (spatially close to the methyl-substituted bridgehead carbon) of **L4**. The results of DFT calculations shed light on disparate coordination modes of **L1–L4** toward the AuCl₃ fragment and explain formation of single coordination products in high yield.

© 2015 Elsevier Ltd. All rights reserved.

1. Introduction

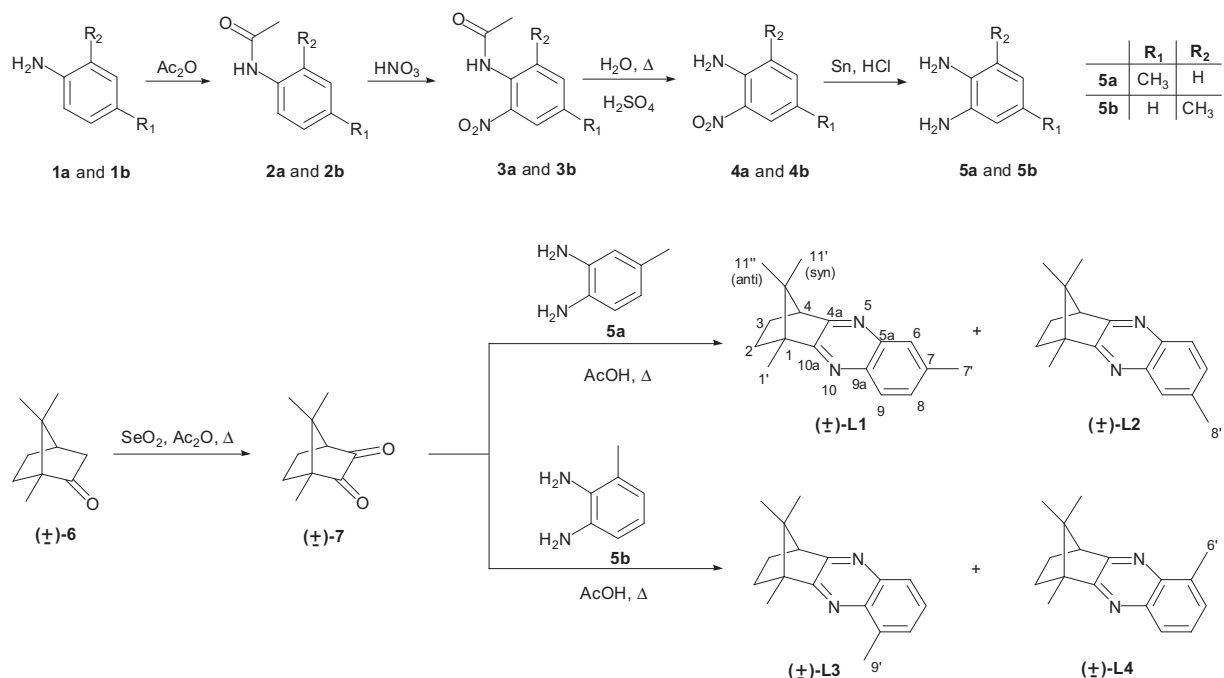
Aromatic nitrogen-containing heterocycles (*N*-heterocycles) are one of the most important classes of ligands in coordination [1–5] and bioinorganic chemistry [6], and have also found use in the rapidly evolving field of metallosupramolecular chemistry [7]. They have been extensively utilized for the formation of numerous mononuclear and polynuclear complexes of different transition metal ions [8–10] and metallosupramolecular assemblies with desirable structures and properties [11]. Moreover, the aromatic *N*-heterocycles have been applied for the construction of structural and functional models of metalloenzyme active sites and other biologically relevant assemblies [12–14]. One of the most interesting molecules within this class of ligands is quinoxaline (qx). Quinoxaline and its derivatives embedded with a variety of functional

groups constitute the building blocks of a wide range of pharmacologically/biologically active compounds [15–22].

Taking into account a broad spectrum of biological activities of quinoxaline, and potential antitumor [23] and antimicrobial [24] properties of gold(III) complexes with *N*-heterocycles, we have recently investigated reactions between [AuCl₄][−] and a wide range of diazaaromatic ligands, such as pyridazine, pyrimidine, pyrazine, quinoxaline and phenazine and found out that they all form mononuclear complexes, in which these ligands act solely as monodentate, regardless of different stoichiometric ratio of the reactants [25,26]. As a continuation of our ongoing interest in the coordination chemistry of gold(III) with diazaaromatics, we decided to investigate the possible coordination of Au(III) ion to four regioisomeric methylcamphorquinoxaline ligands **L1–L4** (1, x, 11, 11-tetramethyl-1,2,3,4-tetrahydro-1,4-methanophenazine, x = 7, 8, 9 or 6, respectively; Scheme 1). Fusion of quinoxaline with camphor made the two metal-binding nitrogen atoms of the quinoxaline core nonequivalent. Such structural ambiguity usually does not result in a single molecular architecture, but different positions (6, 7, 8 or 9) of a methyl-group linked to the aromatic core of camphorquinoxaline could finely tune the coordination ability of **L1–L4** N-atoms. Herein we report the synthesis of four

* Corresponding authors. Tel.: +381 62 80 49 210; fax: +381 18 533 014 (N.S. Radulović). Tel.: +48 61 8291 268; fax: +48 61 829 1555 (U. Rychlewska). Tel.: +381 34 300 251; fax: +381 34 335 040 (M.I. Djuran).

E-mail addresses: nikoradulovic@yahoo.com (N.S. Radulović), urszular@amu.edu.pl (U. Rychlewska), djuran@kg.ac.rs (M.I. Djuran).



Scheme 1. Synthesis, structures and numbering scheme for ligands **L1–L4**. Numbering scheme of C atoms is in agreement with IUPAC recommendations for bridged fused ring systems.

novel regioisomeric methylcamphorquinoxaline ligands **L1–L4** (Scheme 1) and the corresponding mononuclear Au(III)-camphorquinoxaline complexes, **1–4**. All ligands and complexes were studied in detail by 1D and 2D NMR, and gold(III) complexes **1–4** were studied by X-ray diffraction. DFT calculations were conducted to provide better insight into the coordination mode of ligands **L1–L4** toward the AuCl₃ fragment and to explain formation of single coordination products in high yield.

2. Experimental

2.1. Materials

Distilled water was demineralized and purified to a resistance of greater than 10 MΩ/cm. Potassium tetrachloridoaurate(III) (K[AuCl₄]), ethanol (EtOH), dichloromethane (CH₂Cl₂), acetonitrile (CH₃CN), chloroform (CHCl₃), deuterated chloroform (CDCl₃), diethyl ether (Et₂O), hexane (Hex), selenium dioxide (SeO₂), anhydrous magnesium sulfate (MgSO₄), sodium hydroxide (NaOH), *tris*(6,6,7,7,8,8,8-heptafluoro-2,2-dimethyl-3,5-octanedionato)europium(III) (Eu(fod)₃), tetramethylsilane (TMS), *o*-toluidine, *p*-toluidine and Celite® were purchased from Sigma–Aldrich (St. Louis, MS, USA). Sulfuric (H₂SO₄), nitric (HNO₃), hydrochloric (HCl) and acetic (AcOH) acid, as well as, acetic anhydride (Ac₂O), tin (Sn), (±)-camphor, toluene, ethyl acetate (EtOAc) and sodium chloride (NaCl) were supplied by Merck (Darmstadt, Germany). All the employed chemicals were of analytical reagent grade and used without further purification.

2.2. Synthesis of methylcamphorquinoxaline ligands **L1–L4**

The synthesis of ligands **L1–L4** was achieved by the following reaction sequence (Scheme 1).

2.2.1. 4-Methyl-2-nitroaniline (**4a**) and 2-methyl-6-nitroaniline (**4b**)

A slightly modified procedure of Howard was applied [27]. Toluidine (**1a** or **1b**; 53.5 mL, 0.5 mol) was introduced, in small portions and under constant stirring, to Ac₂O (325 mL). The obtained solution was cooled to 12–13 °C in an ice-salt bath. After that, under stirring and at a rate which maintained the temperature within the limits of 10–12 °C, 70% HNO₃ (63 mL) was added dropwise to the reaction mixture. The addition was completed in 2.5 h and the solution was poured, with stirring, into 1.5 L of ice-water. The precipitate (cream-colored solid) of acetamide (**3a**, or mixture of **3b** and **3c**) was collected on a Büchner funnel, washed with four 250-mL portions of ice-water and partially dried by suction. The moist acetamide (**3a**, or mixture of **3b** and **3c**) was mixed with 70% H₂SO₄ (100 mL) and stirred at reflux for 3 h.

The hydrolysis product of acetamide **3b**, 2-methyl-6-nitroaniline (**4b**), was isolated from the reaction mixture by steam distillation. The bright orange needles of **4b**, which separated when the distillate was cooled, were collected on a Büchner funnel and dried in a vacuum desiccator. In the case of the hydrolysis of acetamide **3a**, the warm reaction mixture was diluted with 350 mL of water and made alkaline with 10% *aq.* NaOH. After cooling to room temperature 4-methyl-2-nitroaniline (**4a**) precipitated as a brown powder that was separated by vacuum filtration, washed with three 200-mL portions of water, and dried in a vacuum desiccator. The yield was 53.6% (40.73 g) and 52.3% (39.78 g) for compounds **4a** and **4b**, respectively.

2.2.2. 4-Methylbenzene-1,2-diamine (**5a**) and 3-methylbenzene-1,2-diamine (**5b**)

o-Diamines **5a** and **5b** were obtained following a standard reduction procedure [28]. Twenty-seven milliliters of concentrated HCl were added gradually, through a condenser, to a mixture of 10 g (0.066 mol) of 4-methyl-2-nitroaniline (**4a**) or 2-methyl-6-nitroaniline (**4b**) and 12 g (0.1 mol) of granulated Sn. During the addition of the acid the reaction mixture was vigorously stirred. After that, the reaction mixture was refluxed for 1 h, cooled to

room temperature and made alkaline with a solution of 20 g of NaOH in 33 mL of water.

The reduction product of compound **4b**, 3-methylbenzene-1,2-diamine (**5b**), was isolated from the reaction mixture by steam distillation. Compound **5b** was “salted out” by saturating the distillate with NaCl and extracted with Et₂O. Combined ethereal layers were dried over anhydrous MgSO₄ and concentrated under reduced pressure. Since it was impossible to separate 4-methylbenzene-1,2-diamine (**5a**) by steam distillation, this diamine was directly “salted out” from the reaction mixture and extracted with Et₂O. After the evaporation of the solvent, the crude **5a** was purified by sublimation. The yield was 83.5% (6.72 g) and 85.8% (6.92 g) for compound **5a** and **5b**, respectively.

2.2.3. (±)-Camphorquinone (7)

A modified procedure of White and coworkers was applied [29]. A mixture of (±)-camphor (**6**; 20.0 g, 0.13 mol), SeO₂ (8.0 g, 0.07 mol) and Ac₂O (14.0 mL) was stirred under reflux for 1 h. Then the reaction mixture was cooled to room temperature, and an additional portion of SeO₂ (8.0 g, 0.07 mol) was added. The mixture was again heated to reflux, and two further batches of SeO₂ (8.0 g, 0.07 mol) were added at 2.5-h and 6-h intervals. After the reaction mixture was refluxed for additional 4 h, during that time precipitation of Se was observed, it was cooled to ambient temperature and subsequently 200 mL of EtOAc were added. The gray precipitate was removed by filtration, and the filtrate was diluted with 100 mL of toluene. The filtrate was concentrated under reduced pressure and that yielded crude (±)-camphorquinone as a yellow-orange solid which was then dissolved in 200 mL of EtOAc, and the solution was filtered by vacuum filtration through Celite®. The filtrate was successively washed with 200 mL of 10% aq. NaOH and 100 mL of saturated aq. NaCl solution. The organic layer was dried over anhydrous MgSO₄, filtered, and concentrated *in vacuo* to afford a reasonably pure (according to GC–MS) yellow crystalline (±)-camphorquinone (14 g, 64.1%) which was used in the following reactions without purification.

2.3. 1,x,11,11-Tetramethyl-1,2,3,4-tetrahydro-1,4-methanophenazine (x = 7, 8, 9 and 6 for **L1–L4**, respectively)

A modified procedure of Fitchett and Steel was applied [30]. Camphorquinone (**7**; 3.32 g, 20 mmol) and the corresponding diamine (**5a** or **5b**; 2.44 g, 20 mmol) were refluxed in glacial AcOH (40 mL) for 1 h. The reaction mixture was then neutralised with 10% aq. NaOH and extracted with Et₂O. The combined ethereal extracts, dried over anhydrous MgSO₄, were concentrated under reduced pressure to give a brown oil, which solidified on standing.

The products of condensation of **7** with diamine **5b** (4.30 g, 85.31%), ligands **L3** and **L4**, were separated by column chromatography on SiO₂ applying a Hex:Et₂O (4:1) mixture as the mobile phase. Ligand **L4** was obtained as a colorless crystalline solid, while ligand **L3** formed a pale yellow semi-solid.

Ligands **L1** and **L2** (4.26 g, 84.56%) obtained by the condensation of **7** with diamine **3a** almost completely co-eluted on both the used GC column (HP5-MS) and TLC (SiO₂) plate. TLC was run with a number of mobile phases of varying polarity but with no success in better separating the two ligands. Thus, **L1** and **L2**, were only separated from the unreacted camphorquinone (**7**) and diamine **3a** by “dry-flash” column chromatography using a gradient of Et₂O and Hex (from pure Hex to 10% Et₂O in Hex with an increment step of 5%, v/v). The inseparable mixture of ligands **L1** and **L2** was obtained in the form of a pale yellow powder.

2.3.1. Mixture of 1,7,11,11-tetramethyl-1,2,3,4-tetrahydro-1,4-methanophenazine (**L1**) and 1,8,11,11-tetramethyl-1,2,3,4-tetrahydro-1,4-methanophenazine (**L2**)

M.p. 59.4 °C; R_f = 0.22, Hex:Et₂O (4:1, v/v); RI(HP-5MS) = 2008 (**L2**) and 2010 (**L1**); EI-MS (70 eV), *m/z* (rel. int.): 252 [M]⁺ (91), 237 [M–CH₃]⁺ (48.5), 223 (18.3), 209 (100), 195 (34.9), 182 (4.9), 168 (2.5), 143 (2.8), 128 (1.2), 111 (5.4), 104 (6), 89 (9.9), 77 (3.9), 65 (3.5), 51 (1.8), 41 (3.9). FTIR-ATR (neat) cm⁻¹: 2955 (ν_{as}(CH₃)), 2924 (ν_{as}(CH₂)), 2877 (ν_s(CH₃)), 2866 (ν_s(CH₂)), 1601, 1513 (ν(C_{ar}=C_{ar}) and ν(C_{ar}=N)), 1451 (δ_{as}(CH₃) and δ_{sc}(CH₂)), 1382, 1367 (δ_s(CH₃)), 1332, 1264, 1174, 1106, 1074, 834, 802. UV λ_{max} (CH₃CN) nm (log ε): 316 (3.93), 242 (4.40), 206 (4.70). Anal. Calc. for the mixture = C₁₇H₂₀N₂ (M_r = 252.35); C, 80.91; H, 7.99; N, 11.10. Found: C, 80.62; H, 8.03; N, 11.35%.

2.3.2. 1,9,11,11-Tetramethyl-1,2,3,4-tetrahydro-1,4-methanophenazine (**L3**)

R_f = 0.26, Hex:Et₂O (4:1, v/v); RI(HP-5MS) = 1959; EI-MS (70 eV), *m/z* (rel. int.): 252 [M]⁺ (80.2), 237 [M–CH₃]⁺ (41.5), 223 (17.5), 209 (100), 195 (32.8), 182 (4.5), 168 (2.3), 143 (1.9), 128 (1.3), 116 (3.9), 104 (4.5), 89 (9.6), 77 (3.4), 65 (3.2), 51 (1.5), 41 (3.6). FTIR-ATR (neat) cm⁻¹: 2958 (ν_{as}(CH₃)), 2925 (ν_{as}(CH₂)), 2871 (ν_s(CH₃) and ν_s(CH₂)), 1587, 1513, 1474 (ν(C_{ar}=C_{ar}) and ν(C_{ar}=N)), 1451 (δ_{as}(CH₃) and δ_{sc}(CH₂)), 1391, 1371 (δ_s(CH₃)), 1329, 1263, 1173, 1110, 1079, 796, 762; UV λ_{max} (CH₃CN) nm (log ε): 316 (3.86), 243 (4.52), 204 (4.64). Anal. Calc. for **L3** = C₁₇H₂₀N₂ (M_r = 252.35); C, 80.91; H, 7.99; N, 11.10. Found: C, 80.73; H, 7.95; N, 11.32%.

2.3.3. 1,6,11,11-Tetramethyl-1,2,3,4-tetrahydro-1,4-methanophenazine (**L4**)

M.p. 82.9 °C; R_f = 0.36, Hex:Et₂O (4:1, v/v); RI(HP-5MS) = 1973; EI-MS (70 eV), *m/z* (rel. int.): 252 [M]⁺ (92.7), 237 [M–CH₃]⁺ (50.4), 223 (18.4), 209 (100), 195 (34.6), 182 (4.7), 168 (2.6), 143 (2.2), 128 (1.3), 116 (4), 104 (4.6), 89 (9.6), 77 (3.3), 65 (2.9), 51 (1.4), 41 (3.2). FTIR-ATR (neat) cm⁻¹: 2956 (ν_{as}(CH₃)), 2925 (ν_{as}(CH₂)), 2868 (ν_s(CH₃) and ν_s(CH₂)), 1587, 1513 (ν(C_{ar}=C_{ar}) and ν(C_{ar}=N)), 1474, 1449 (δ_{as}(CH₃) and δ_s(CH₂)), 1389, 1370 (δ_s(CH₃)), 1264, 1171, 1118, 1093, 1069, 793, 760. UV λ_{max} (CH₃CN) nm (log ε): 316 (3.93), 244 (4.58), 204 (4.71). Anal. Calc. for **L4** = C₁₇H₂₀N₂ (M_r = 252.35); C, 80.91; H, 7.99; N, 11.10. Found: C, 81.04; H, 7.85; N, 11.11%.

Retention data for all synthetic intermediates are given in Table S1.

2.4. Synthesis of the gold(III) complexes **1–4**

Gold(III) complexes with ligands **L1–L4** were synthesized according to the modified procedure published in the literature for the preparation of [AuCl₃(N-heterocycle)] complexes (heterocycle is the monodentate pyridazine, pyrimidine, pyrazine, quinoxaline and phenazine) [25,26].

The solution of 0.5 mmol of a solid mixture, which contained approximately equal amounts of **L1** and **L2** (0.55:0.45 M ratio, according to a ¹H NMR analysis), as well as, separately, of ligands **L3** and **L4** (126.2 mg) in 10.0 mL of ethanol was added slowly under stirring to the solution containing an equimolar amount of K[AuCl₄] (188.9 mg in 10.0 mL of ethanol). The resulting yellow solution was stirred in the dark at ambient temperature for 24 h. The yellow precipitate, formed after standing of this solution in a refrigerator overnight, was filtered off, washed with water and then recrystallized from dichloromethane to form yellow crystals of gold(III) complexes. These crystals were collected from the solution and dried in the dark at ambient temperature. The pure complexes of **L1** and **L2** with Au(III), [AuCl₃(**L1**)] (**1**) and [AuCl₃(**L2**)] (**2**), were isolated by the means of a fractional crystallization from

chloroform. The yield was 72% for the mixture of [AuCl₃(**L1**)] (**1**) and [AuCl₃(**L2**)] (**2**) (200.0 mg; both complexes have the same molecular formula, thus allowing us to calculate the yield), 82% for [AuCl₃(**L3**)] (**3**) (227.8 mg) and 78% for [AuCl₃(**L4**)] (**4**) (216.7 mg). *Anal. Calc.* for [AuCl₃(**L1–L4**)] = C₁₇H₂₀AuCl₃N₂ (*M_r* = 555.68); C, 36.74; H, 3.63; N, 5.04. Found for [AuCl₃(**L3**)]: C, 36.52; H, 3.53; N, 5.04%. Found for [AuCl₃(**L4**)]: C, 37.70; H, 3.65; N, 5.16%.

2.4.1. Mixture of [AuCl₃(**L1**)] (**1**) and [AuCl₃(**L2**)] (**2**)

FTIR-ATR (neat) cm⁻¹: 2958 (*v*_{as}(CH₃)), 2929 (*v*_{as}(CH₂)), 2870 (*v*_s(CH₃) and *v*_s(CH₂)), 1610, 1513 (*v*(C_{ar}=C_{ar}) and *v*(C_{ar}=N)), 1446 (*δ*_{as}(CH₃) and *δ*_{sc}(CH₂)), 1393, 1373 (*δ*_s(CH₃)), 1333, 1275, 1104, 1078, 811.

2.4.2. [AuCl₃(**L3**)] (**3**)

FTIR-ATR (neat) cm⁻¹: 2953 (*v*_{as}(CH₃)), 2924 (*v*_{as}(CH₂)), 2873 (*v*_s(CH₃) and *v*_s(CH₂)), 1621, 1510 (*v*(C_{ar}=C_{ar}) and *v*(C_{ar}=N)), 1466 (*δ*_{as}(CH₃) and *δ*_{sc}(CH₂)), 1394, 1375(*δ*_s(CH₃)), 1345, 1277, 1161, 1118, 1068, 748, 721.

2.4.3. [AuCl₃(**L4**)] (**4**)

FTIR-ATR (neat) cm⁻¹: 2952 (*v*_{as}(CH₃)), 2925 (*v*_{as}(CH₂)), 2868 (*v*_s(CH₃) and *v*_s(CH₂)), 1587, 1513 (*v*(C_{ar}=C_{ar}) and *v*(C_{ar}=N)), 1474, 1449 (*δ*_{as}(CH₃) and *δ*_{sc}(CH₂)), 1389, 1370 (*δ*_s(CH₃)), 1264, 1171, 1118, 1093, 1069, 793, 760.

2.5. Measurements

2.5.1. FTIR, UV and elemental analyses and measurement of melting points

The IR measurements (ATR – attenuated total reflectance) were carried out using a Thermo Nicolet model 6700 FTIR instrument (Waltham, USA). UV spectra (in CH₃CN) were measured using a UV-1800 UV-Vis spectrophotometer (Shimadzu, Kyoto, Japan). Melting points were determined on MPM-HV2 melting point meter (Paul Marienfeld GmbH & Co. KG, Lauda-Königshofen, Germany). Elemental microanalyses for carbon, hydrogen and nitrogen of the synthesized methylcamphorquinoline ligands and gold(III) complexes were performed by the Microanalytical Laboratory, Faculty of Chemistry, University of Belgrade.

2.5.2. GC-MS, TLC and LC analyses

GC-MS analyses of all samples (synthetic intermediates, chromatographic fractions and ligands) were repeated three times using a Hewlett–Packard 6890N gas chromatograph. The gas chromatograph was equipped with a fused silica capillary column HP-5MS (5% phenylmethylsiloxane, 30 m × 0.25 mm, film thickness 0.25 μm; Agilent Technologies, Santa Clara, CA, USA) and coupled with a 5975B mass selective detector from the same company. The injector and interface were operated at 250 and 300 °C, respectively. The oven temperature was raised from 70 to 290 °C at a heating rate of 5 °C/min and then isothermally held for 10 min. Helium at 1.0 mL/min was used as a carrier gas. 1 μL of the solution of the corresponding compound/mixture in diethyl ether (1:100, w/v or v/v), were injected in a pulsed split mode (the flow was 1.5 mL/min for the first 0.5 min and then set to 1.0 mL/min throughout the remainder of the analysis; split ratio 40:1). The mass selective detector was operated at the ionization energy of 70 eV, in the 35–700 amu range, with a scanning speed of 0.34 s.

TLC analyses were performed on alumina-backed silica gel 40 F254 plates (Merck, Darmstadt, Germany). The spots on TLC were visualized by UV light (254 nm) and by spraying with phosphomolybdic acid (12 g) in EtOH (250 mL) followed by heating. Preparative chromatographic separations (column chromatography) were carried out using silica gel 60 (particle size distribution

40–63 μm) obtained from Carl Roth GmbH + Co.KG (Karlsruhe, Germany).

2.5.3. NMR measurements

All NMR spectra were recorded at 25 °C in deuterated chloroform with TMS as internal standard. Chemical shifts (*δ*) are reported in parts per million and referenced to TMS (*δ*_H = 0.00 ppm) in ¹H and ¹³C NMR spectra and/or to solvent protons (deuterated chloroform: *δ*_H = 7.25 ppm and *δ*_C = 77 ppm) in heteronuclear 2D spectra. Scalar couplings are reported in Hertz (Hz). Samples (ca. 20–30 mg of ligands and complexes) were dissolved in 1 mL of deuterated chloroform, and 0.7 mL of the solution transferred into a 5 mm Wilmad, 528-TR-7 NMR tube.

The ¹H and ¹³C NMR spectra were recorded on a Bruker Avance III 400 MHz NMR spectrometer (Fällanden, Switzerland; ¹H at 400 MHz, ¹³C at 101 MHz), equipped with a 5-mm dual ¹³C/¹H probe head. The ¹H NMR spectra were recorded with 16 scans, 1 s relaxation delay, 4 s acquisition time, 0.125 Hz digital FID resolution, 51 280 FID size, with 6410 Hz spectral width, and an overall data point resolution of 0.0003 ppm. The ¹³C NMR spectra were recorded with Waltz 161H broadband decoupling, 12000 scans, 0.5 s relaxation delay, 1 s acquisition time, 0.5 Hz digital FID resolution, 65536 FID size, 31850 Hz spectral width, and an overall data point resolution of 0.005 ppm. Standard pulse sequences were used for 2D spectra. ¹H–¹H gDQCOSY and NOESY spectra were recorded at spectral widths of 5 kHz in both F2 and F1 domains; 1 K × 512 data points were acquired with 32 scans per increment and the relaxation delays of 2.0 s. The mixing time in NOESY experiments was 1 s. Data processing was performed on a 1 K × 1 K data matrix. Inverse detected 2D heteronuclear correlated spectra were measured over 512 complex points in F2 and 256 increments in F1, collecting 128 (gHMBC) or 256 (¹H–¹³C gHMBC) scans per increment with a relaxation delay of 1.0 s. The spectral widths were 5 and 27 kHz in F2 and F1 dimensions, respectively. The gHMBC experiments were optimized for C–H couplings of 165 Hz; the ¹H–¹³C gHMBC experiments were optimized for long-range C–H couplings of 10 Hz. Fourier transforms were performed on a 512 × 512 data matrix. $\pi/2$ shifted sine-squared window functions were used along F1 and F2 axes for all 2D spectra.

2.6. Crystallographic data collection and refinement of the structures

Crystals of **1** and **2** displayed very weak X-ray diffraction. In order to improve their scattering ability, the X-ray measurements for these compounds were carried out at 120 K, while the X-ray measurements for **3** and **4** were carried out at 295 K. All measurements were done using the Mo K α radiation (λ = 0.71073 Å) on Xcalibur kappa-geometry diffractometer equipped with Eos CCD detector using CrysAlisPro software [31]. Empirical absorption correction using spherical harmonics, implemented in SCALE3 ABSPACK scaling algorithm, was also applied [32]. Inspection of the Ewald sphere clearly indicated that in the case of crystals **1** and **2**, we dealt with partially powdered material and this had a direct effect on the quality of the X-ray measurements. Further crystallographic and refinement data can be found in Table 1. The structures were solved by direct methods using SHELXS-86 [33] and refined by full-matrix least-squares calculations on *F*² with SHELXL [33]. Anisotropic displacement parameters were refined for all non-hydrogen atoms. The positions of the hydrogen atoms attached to the carbon atoms were calculated at standardized distances specified in the SHELXL program and refined using a riding model with isotropic displacement parameters 20% higher than the isotropic equivalent of their carriers. MERCURY [34] computer graphics program was used to prepare drawings. Because the diffraction patterns for **1** and **2** showed signs of the presence of partially powdered material, the residual electron density maps

still display significant minima and maxima, which could not be accounted for. Moreover, in the crystal of **2** the camphor part of the ligand is statically disordered over two positions, the ratio of the major and minor components being 0.70:0.30.

2.7. Quantum-mechanical calculations

The M06 [35], M06-2X [35] and B3LYP [36,37] density functional theory methods were employed in our calculations. The B3LYP and M06 methods are known to give good descriptions of transition metal complexes [35,38–40], while the M06-2X are recommended for the aromatic nitrogen-containing heterocycles [41]. The basis set for calculations on gold(III) complexes was composed: Dunning's correlation consistent polarized valence double- ζ (cc-pVDZ) basis set for the hydrogen, nitrogen, oxygen and chlorine [42,43] and LanL2TZ(f) basis set for the gold atoms [44]. The latter contains the LanL2 relativistic effective core potential (RECP) of Hay and Wadt [44] and a flexible triple- ζ basis set augmented with f polarization functions in the treatment of valence shell on the Au atom. To take into account the effect of the solvent, the Polarizable Continuum Model (PCM) [45] was used with ethanol chosen as the solvent as in synthesis of the complexes and chloroform for the conduct of the ligands and complexes during NMR measurements. All structures were fully optimized without any geometric constraints. The optimized structures were confirmed to be potential energy minima by vibrational frequency calculations at the same level of theory, because no imaginary frequencies were found. To check the influence of basis set effects, for each optimized geometry both in the gas phase and the solvent ethanol, additional single-point calculations were completed at the M06-2X/(LanL2TZ(f)+cc-PVTZ) level of theory (cc-PVTZ is the correlation consistent polarized valence triple- ζ basis set [42,43]). Starting from the optimized geometries of **L1–L4** and gold(III) complexes **1–4**, their chemical shifts and coupling constants were calculated using GIAO method [46] with B3LYP density functional (SDD basis set [47]). Finally, the natural bond analyses (NBO) [48] were performed at M06-2X/cc-PVTZ and M06-2X/(LanL2TZ

(f)+cc-PVTZ) levels of theory in order to provide indices of the ligands and gold(III) complexes, respectively.

All DFT calculations were performed using the Gaussian 09 program package [49]. The M06, M06-2X and B3LYP methods, as well as cc-pVDZ, cc-PVTZ and SDD basis sets were employed as implemented in the software package, while the LanL2TZ(f) basis set for gold was obtained from EMSL Basis set Exchange (<https://bse.pnl.gov/bse/portal>).

3. Results and discussion

3.1. Ligand design and synthesis

Structurally related camphor-diaza-heteroaromatic fused hybrids were previously used for the preparation of coordination compounds of zinc [30,50], copper [30], silver [51] and mercury

Table 2
Selected geometrical parameters (Å/°) in complexes **1–4**.

	1	2	3	4
Au1–N	2.043(5)	2.084(14)	2.040(3)	2.046(3)
Au1–Cl1	2.2880(18)	2.281(5)	2.2640(9)	2.2682(10)
Au1–Cl2	2.2631(16)	2.259(4)	2.2573(9)	2.2635(9)
Au1–Cl3	2.2635(17)	2.272(5)	2.2726(9)	2.2796(9)
N1–C5	1.304(8)	1.25(2)	1.304(4)	1.290(4)
N1–C6	1.383(8)	1.41(2)	1.392(4)	1.370(4)
N2–C11	1.386(8)	1.35(2)	1.382(4)	1.396(4)
N2–C12	1.304(8)	1.32(2)	1.300(4)	1.303(4)
C1–C13	1.502(9)	1.46(3)	1.514(5)	1.495(5)
		1.54(2)		
C9–C17	1.497(10)	1.48(2)	1.492(5)	1.486(5)
N–Au1–Cl2	177.28(15)	178.4(4)	174.93(7)	176.79(7)
N–Au1–Cl1	88.26(15)	88.8(4)	88.52(7)	88.90(8)
N–Au1–Cl3	88.48(15)	87.8(4)	88.94(7)	88.63(8)
Cl1–Au1–Cl2	92.55(7)	91.19(17)	91.26(4)	90.76(4)
Cl1–Au1–Cl3	176.65(6)	176.59(17)	177.21(4)	176.62(4)
Cl2–Au1–Cl3	90.75(7)	92.20(18)	91.37(4)	91.84(4)
<i>Angles between vectors (°)</i>				
N···N/Au···Cl2	3.4	2.6	9.6	3.2

Table 1
Crystal data for **1–4**.

	1	2	3	4
<i>Crystal data</i>				
Crystal system, space group	monoclinic, $P2_1/c$	orthorhombic, $Pbca$	triclinic, $P\bar{1}$	triclinic, $P\bar{1}$
T (K)	120	120	295	295
a, b, c (Å)	9.7252(2), 9.0731(2), 20.8344(5)	14.3994(6), 13.8518(5), 18.5371(12)	9.8377(2), 10.3018(2), 10.5915(2)	10.1252(2), 10.2596(2), 10.4262(2)
α (°)	90	90	113.768(2)	92.686(2)
β (°)	96.242(2)	90	107.777(2)	107.263(2)
γ (°)	90	90	92.197(1)	113.411(2)
V (Å ³)	1827.48(7)	3697.4(3)	919.28(4)	932.22(4)
Z	4	8	2	2
μ (mm ⁻¹)	8.49	8.39	8.44	8.32
Crystal size (mm)	0.50 × 0.50 × 0.03	0.20 × 0.10 × 0.10	0.22 × 0.20 × 0.10	0.25 × 0.20 × 0.10
<i>Data collection</i>				
$T_{\text{minimum}}, T_{\text{maximum}}$	0.558, 1.000	0.538, 1.000	0.580, 1.000	0.329, 1.000
No. of measured, independent and observed [$I > 2\sigma(I)$] reflections	17538, 3218, 3001	44877, 3252, 2422	24032, 3253, 3160	25564, 3287, 3157
R_{int}	0.037	0.113	0.023	0.025
$(\sin \theta/\lambda)_{\text{max}}$ (Å ⁻¹)	0.595	0.595	0.595	0.595
<i>Refinement</i>				
$R[F^2 > 2\sigma(F^2)], wR(F^2), S$	0.032, 0.068, 1.30	0.078, 0.215, 1.10	0.016, 0.038, 1.11	0.017, 0.042, 1.07
No. of reflections	3218	3252	3253	3287
No. of parameters	212	240	212	212
No. of restraints	0	84	0	2
	$w = 1/[\sigma^2(F_o^2) + (0.0109P)^2 + 11.6046P]$ where $P = (F_o^2 + 2F_c^2)/3$	$w = 1/[\sigma^2(F_o^2) + (0.0869P)^2 + 157.7844P]$ where $P = (F_o^2 + 2F_c^2)/3$	$w = 1/[\sigma^2(F_o^2) + (0.0172P)^2 + 0.9164P]$ where $P = (F_o^2 + 2F_c^2)/3$	$w = 1/[\sigma^2(F_o^2) + (0.0205P)^2 + 1.0838P]$ where $P = (F_o^2 + 2F_c^2)/3$
$\Delta\rho_{\text{maximum}}, \Delta\rho_{\text{minimum}}$ (e Å ⁻³)	1.31, -2.08	4.45, -2.14	0.73, -0.35	0.98, -0.41

[50]. It was observed that this type of ligands preferably coordinates through the less hindered nitrogen atom [30], however, the products of coordination *via* nitrogen spatially close to the bridge-head methyl-group have also been obtained [51]. To the best of our knowledge, Au(III) coordination compounds with camphor-fused diaza heteroaromatic ligands were not previously reported. Considering this, we prepared four regioisomeric methylcamphorquinoxaline ligands **L1–L4**, by following the reaction sequence given in Scheme 1 [27–30], and synthesized their mononuclear complexes with Au(III) (complexes **1–4**). 3- and 5-methylbenzenediamines (**5a** and **5b**; prepared by the nitration of *o*- or *p*-toluidine, followed by the reduction of the nitro-group) were condensed with (\pm)-camphorquinone, which was, in turn, prepared by a SeO₂ oxidation of (\pm)-camphor. In this way, we obtained mixtures of **L1/L2** and **L3/L4** ligands. The mixture of **L3** and **L4** isomers was successfully separated using column chromatography on SiO₂ (for details, see Experimental section). We tried to separate **L1** and **L2** in a similar manner, but they co-eluted in a number of different mobile phases. For this reason, in all further experiments (the synthesis of Au(III) complexes and NMR analyses), we used the mixture of **L1** and **L2** ligands in 0.55:0.45 M ratio established on the basis of the ¹H NMR spectra. Luckily, the pure Au(III) complexes of **L1** and **L2** were isolated by means of fractional crystallization from chloroform. Interestingly,

although we used an almost equimolar mixture of **L1** and **L2**, the obtained mixture of complexes was enriched in **1** (based on ¹H NMR, **1** and **2** were found to be in the 0.8:0.2 M ratio, respectively). This might be explained either by (a) different solubilities of **1** and **2** in ethanol (reaction of **L1** and **L2** with K[AuCl₄] was conducted in this solvent), (b) rates of their formation or, alternatively, (c) coordination abilities of **L1** and **L2**, *i.e.* thermodynamic stability of **1** and **2**. It is also important to note that regardless of the different stoichiometric ratio of the reactants used ($n(\text{K}[\text{AuCl}_4]):n(\text{L1–L4}) = 2:1, 1:1$ or $1:2$, respectively), all reactions led to the formation of only mononuclear gold(III) complexes **1–4**. All obtained gold(III) complexes **1–4** were further studied by X-ray diffraction. A complete assignment of ¹H and ¹³C resonances was accomplished for both the complexes and the ligands through a careful analysis of 1D/2D NMR spectra.

3.2. Description of the single crystal structures

Details of the data collection parameters and refinement of the structures of **1–4** are presented in Table 1. Key geometrical parameters for these complexes have been included in Table 2, while their molecular topology, as present in crystals, is displayed in Fig. 1 and compared in Fig. 2, which is the least-squares fit of all

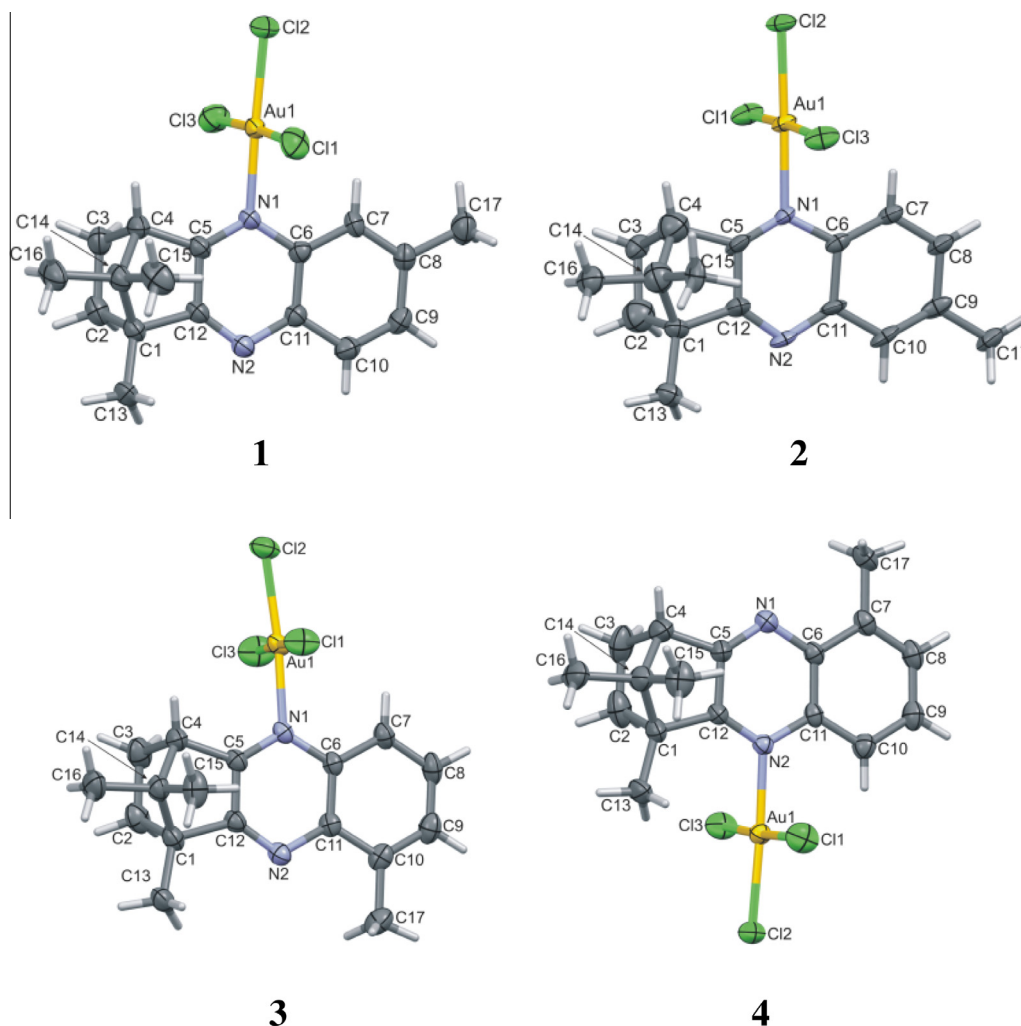


Fig. 1. Perspective view of the investigated gold(III) complexes **1–4** as present in crystals, showing atom numbering and atomic displacement parameters at 40% probability level (H-atoms were drawn in an arbitrary scale). All crystal structures are centrosymmetric, so both enantiomers are present in equal amounts, while only one of them, namely the 1*R*, 4*S* isomer, is displayed. Only one of the two components of disorder in the crystal structure of **2** is displayed.

four gold(III) complexes. The investigated crystals contain an equimolar amount of enantiomeric complex molecules.

The crystal structure of all four complexes consists of discrete monomeric species with the Au(III) in a square planar coordination geometry and one Au–N(L1–L4) and three Au–Cl bonds. The angle between the pyrazine moiety and the plane defined by the four donor atoms surrounding the Au(III) ion is close to 90° and amounts to 80.65(13), 86.6(4), 87.48(8) and 85.98(8)° in **1**, **2**, **3** and **4**, respectively (Fig. 2). In all these complexes, the Au–Cl2 bond *trans* to the coordinated nitrogen is the shortest of the Au–Cl bonds (Table 2), although the differences are relatively small. Each of the ligands L1–L4 coordinates through only one nitrogen atom, while the remaining nitrogen atom is non-coordinating (Fig. 1). The two ligand nitrogen atoms are nonequivalent; one lies in the neighborhood of an unsubstituted bridgehead C-atom (labeled as N1 in all structures)¹, while the other (N2) is positioned close to the methyl-substituted bridgehead carbon of the camphor moiety. It turns out that in **1–3**, the ligand molecules coordinate through the less hindered nitrogen atom N1, while in **4** via N2. The change in the coordination site of **4** is connected with the presence of a bulky methyl group attached to the aromatic ring, in the nearest proximity of its N1 atom. This suggests that methyl group attached to the proximal aromatic ring might exert bigger steric hindrance than the methyl group attached to the proximal Csp³ carbon, presumably due to the longer Csp³–Csp² single bond (C1–C12 1.506 (5) Å), than the aromatic bond (C6–C7 1.419(4) Å). The same reasoning can be applied to rationalize a tendency of the C–H group of aromatic ring to approach the Au(III) ion at much shorter distance than its aliphatic analog. More specifically, in **1**, there is a short intramolecular Au···H contact of 2.69 Å with the benzene hydrogen, while the analogous distance to the methine hydrogen is significantly longer (3.05 Å). The analogous values in **2** are 2.78 and 3.04 Å, while in **3** they are more equalized (2.82 versus 2.94 Å). In **4** the Au···H–C(aromatic) contact of 2.69 Å is comparable in length with the shortest of the Au···H contacts involving the camphor methyl group (2.67 Å). Quite unexpectedly, the N–Au–Cl(*trans*) valence angle in **3** deviates significantly from 180° being only 174.93(7)°, while in the remaining complexes **1**, **2** and **4**, it amounts to 177.28 (15), 178.5(4) and 176.79(7)°, respectively. Selected geometrical parameters describing the complex molecules **1–4** are listed in Table 2.

Packing in crystals is governed by weak CH···Cl hydrogen bonds and van der Waals interactions. Not surprisingly the uncoordinated nitrogen atoms are not engaged in any intermolecular interactions.

3.3. NMR spectroscopic characterization

In order to get an insight into the solution chemistry of Au(III) coordination compounds with L1–L4, alongside the crystallographic one, we performed detailed 1D and 2D NMR analyses of **1–4** and of the corresponding ligands L1–L4. All NMR experiments were performed with CDCl₃ solutions of the ligands and complexes, and the results are summarized in Tables 3 and 4.

The complete assignment of both ¹H and ¹³C NMR was based on 2D NMR (¹H–¹H gDQCOSY, NOESY, ¹H–¹³C gHSQC and ¹H–¹³C gHMBC) and a series of selective homodecoupling experiments. The most important observed HMBC and NOE correlations for **L3**, that allowed the assignment, are summarized in Fig. 3 and were analogous to that observed for the other studied compounds (all observed HMBC interactions for L1–L4 and **1–4** are given in Table S2). In the case of L1–L4, the assignment of signals corresponding to quaternary C-atoms, C-1 and C-11, were additional

confirmed by NMR experiments with lanthanide-induced shift reagent Eu(fod)₃, tris(6,6,7,7,8,8,8-heptafluoro-2,2-dimethyl-3,5-octanedionato)europium(III). The chemical shift of the signal corresponding to C-1 was more susceptible to the addition of the shift reagent (higher value of the slope of the corresponding linear dependence). In the proton spectra of L1–L4, protons H-2_{exo}, H-2_{endo}, H-3_{exo}, H-3_{endo} and H-4 formed a second-order spin system (ABHMX; Pople notations for these atoms are defined in Table 3). Thus, with the exception of H-4 (a broad doublet), the chemical shifts and coupling constant for these nuclei (signals represented complex multiplets that were for L1–L3 H-2_{endo} and H-2_{exo} even partially overlapped), could not be directly retrieved from the proton spectra. However upon auration, these signals became well resolved first-order multiplets in the corresponding complexes **1–4**. In order to resolve the L1–L4 second-order spin system multiplets, we used the HiFSA-approach (¹H iterative Full Spin Analysis) [52]. Starting from the optimized geometries of L1–L4 (Figs. S1 and S2), we calculated the chemical shifts and coupling constants of H-2_{exo/endo}, H-3_{exo/endo} and H-4 proton using GIAO method [46] with B3LYP density functional [36,37] (SDD basis set [47]); the effect of solvent (NMR spectra were recorded in chloroform-*d*) was taken into account by employing the Polarizable Continuum Model (PCM) [45]. After that, the predicted δ_H and *J* values were manually adjusted, using the (preliminary) chemical shifts/coupling constants obtained during 1D/2D NMR analysis of ligands and complexes.

Subsequent optimization using WINDNMR software [53] led to a systematic refinement of all calculated NMR parameters until the simulation outcome was in excellent agreement with the experimental data. The calculated and experimentally observed ¹H NMR signals of L3/L4 H-2_{exo}, H-2_{endo}, H-3_{exo} and H-3_{endo} are given in parallel in Figs. S3 and S4. The HiFSA-approach allowed us to determine the exact values of the chemical shifts and coupling constants for the second-order spin system nuclei (see Captions to Figs. S3 and S4). For **L3**, δ_H (ppm) were 2.280, 2.036, 1.397 and 1.396 (for H-3_{exo} (M), H-2_{exo} (H), H-2_{endo} (B), H-3_{endo} (A),

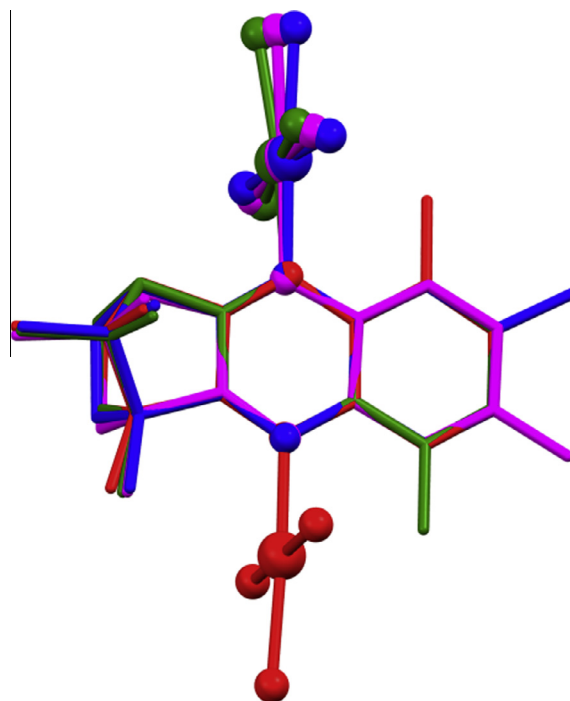


Fig. 2. Least squares fit of the four complex molecules as present in crystals. **1** – blue, **2**–pink, **3**– green, **4**– red. (Color online.)

¹ The numbering of atoms in **1–4** applied in the X-ray studies does not match the one applied in the NMR and DFT studies, which follow the IUPAC recommendation.

Table 3
¹H chemical and coordination shifts (in parentheses), alongside multiplicities and coupling constants (*J*_{H-H}), for the ligands **L1–L4** and the corresponding gold(III) complexes **1–4** in CDCl₃.

	L1 ^a	[AuCl ₃ (L1)] (1) ^b	L2 ^a	[AuCl ₃ (L2)] (2) ^c	L3	[AuCl ₃ (L3)] (3)	L4	[AuCl ₃ (L4)] (4)
H-2 _{exo}	2.10–1.96, m, ABHM _X ^d	2.19, ddd, <i>J</i> = 13.1, 11.0, 4.4 Hz (+0.16)	2.10–1.96, m, ABHM _X	2.19, ddd, <i>J</i> = 13.1, 11.0, 4.4 Hz (+0.16)	2.09–1.98, m, ABHM _X	2.21, ddd, <i>J</i> = 13.1, 11.2, 4.3 Hz (+0.17)	2.10–2.00, m, ABHM _X	2.20, ddd, <i>J</i> = 13.8, 11.0, 4.2 Hz (+0.15)
H-2 _{endo}	1.40–1.34, m, ABHM _X ^d	1.52, ddd, <i>J</i> = 13.1, 9.2, 4.5 Hz (+0.12)	1.40–1.34, m, ABHM _X	1.52, ddd, <i>J</i> = 13.1, 9.2, 4.5 Hz (+0.12)	1.39–1.35, m, ABHM _X	1.53, ddd, <i>J</i> = 13.1, 9.1, 4.3 Hz (+0.16)	1.41–1.36, m, ABHM _X	1.90, ddd, <i>J</i> = 13.8, 9.3, 4.2 Hz (+0.52)
H-3 _{exo}	2.37–2.21, m, ABHM _X ^d	2.50, ddt, <i>J</i> = 13.6, 11.0, 4.5 Hz (+0.21)	2.37–2.21, m, ABHM _X	2.50, ddt, <i>J</i> = 13.6, 11.0, 4.5 Hz (+0.21)	2.36–2.21, m, ABHM _X	2.51, pdtd, <i>J</i> = 13.2, 11.2, 4.6, 4.3 Hz (+0.22)	2.33–2.23, m, ABHM _X	2.40, ddt, <i>J</i> = 13.2, 11.0, 4.2 Hz (+0.12)
H-3 _{endo}	1.45–1.40, m, ABHM _X ^d	1.77, ddd, <i>J</i> = 13.6, 9.2, 4.3 Hz (+0.45)	1.45–1.40, m, ABHM _X	1.77, ddd, <i>J</i> = 13.6, 9.2, 4.3 Hz (+0.45)	1.44–1.40, m, ABHM _X	1.77, ddd, <i>J</i> = 13.2, 9.1, 4.3 Hz (+0.44)	1.45–1.41, m, ABHM _X	1.51, ddd, <i>J</i> = 13.2, 9.3, 4.2 Hz (+0.08)
H-4	3.04, bd, <i>J</i> = 4.4 Hz, ABHM _X ^d	3.83, bd, <i>J</i> = 4.6 Hz (+0.79)	3.04, bd, <i>J</i> = 4.4 Hz, ABHM _X	3.81, bd, <i>J</i> = 4.7 Hz (+0.79)	3.04, d, <i>J</i> = 4.5 Hz, ABHM _X	3.84, d, <i>J</i> = 4.6 Hz (+0.80)	3.10, bd, <i>J</i> = 4.4 Hz, ABHM _X	3.35, bd, <i>J</i> = 4.2 Hz (+0.25)
H-6	7.76, dq, <i>J</i> = 1.5, 0.5 Hz	8.32, bs (+0.56)	7.86, bd, <i>J</i> = 8.4 Hz	8.46, dq, <i>J</i> = 8.6 Hz (+0.60)	7.82, ddq, <i>J</i> = 8.0, 1.9, 0.5 Hz	8.42, bd, <i>J</i> = 8.4, 1.2, 0.5 Hz (+0.60)	–	–
H-7	–	–	7.47, ddq, <i>J</i> = 8.4, 1.5, 0.5, Hz	7.77, ddq, <i>J</i> = 8.8, 1.8, 0.4 Hz (+0.30)	7.51, dd, <i>J</i> = 8.0, 7.2 Hz	7.83, dd, <i>J</i> = 8.4, 7.3 Hz (+0.32)	7.47, ddq, <i>J</i> = 7.1, 1.8, 0.9 Hz	7.75, ddq, <i>J</i> = 7.4, 1.0, 0.8 Hz (+0.28)
H-8	7.47, ddq, <i>J</i> = 8.4, 1.5, 0.5 Hz	7.72, ddq, <i>J</i> = 8.5, 1.4, 0.4 Hz (+0.25)	–	–	7.47, ddq, <i>J</i> = 7.2, 1.8, 0.8 Hz	7.75, dq, <i>J</i> = 7.3, 0.8 Hz (+0.28)	7.51, dd, <i>J</i> = 8.0, 7.1 Hz	7.84, dd, <i>J</i> = 8.5, 7.4 Hz (+0.33)
H-9	7.92, bd, <i>J</i> = 8.4 Hz	8.10, bd, <i>J</i> = 8.5 Hz (+0.18)	7.83, dq, <i>J</i> = 1.5, 0.5 Hz	8.01, bs (+0.18)	–	–	7.88, ddq, <i>J</i> = 8.0, 1.8, 0.6 Hz	8.67, ddq, <i>J</i> = 8.5, 1.5, 0.9 Hz (+0.79)
H-1', CH ₃	1.43, s	1.48, s (+0.05)	1.43, s	1.48, s (+0.05)	1.42, s	1.50, s (+0.08)	1.44, s	2.23, s (+0.79)
H-7'/8'/9'/ 6', CH ₃	2.55, bs	2.70, bs (+0.15)	2.55, bs	2.64, bs (+0.09)	2.79, bs	2.88, bs (+0.09)	2.79, bs	2.84, bs (+0.05)
H-11' (<i>syn</i>), CH ₃	0.62, s	0.74, s (+0.12)	0.62, s	0.74, s (+0.12)	0.61, s	0.77, s (+0.16)	0.61, s	0.78, s (+0.17)
H-11'' (<i>anti</i>), CH ₃	1.11, s	1.20, s (+0.09)	1.11, s	1.20, s (+0.09)	1.11, s	1.24, s (+0.13)	1.11, s	1.20, s (+0.09)

^a **L1** and **L2** chemical shifts and coupling constants were determined by 1D/2D NMR analyses of mixture of ligands **L1** and **L2**.

^b The results of the NMR analyses of pure [AuCl₃(**L1**)], which was isolated by fractional crystallization of [AuCl₃(**L1**)]/[AuCl₃(**L2**)] mixture from deuterated chloroform.

^c [AuCl₃(**L2**)] chemical shifts and coupling constants were determined by 1D/2D NMR analyses of [AuCl₃(**L1**)]/[AuCl₃(**L2**)] mixture.

^d In the ligands, H-2_{exo}, H-2_{endo}, H-3_{exo}, H-3_{endo} and H-4 protons form a second-order ABHM_X spin coupling system (Pople notation of the corresponding nuclei is underscored); bd-broad doublet, bs-broad singlet, d-doublet, dd-doublet of doublets, ddd-doublet of doublet of doublets, ddt-doublet of doublet of triplets, ddq-doublet of doublet of quartets, dq-doublet of quartets, m-multiplet, pdtd-pseudo doublet of doublet of triplets, qd-quartet of doublets, s-singlet.

Table 4
¹³C chemical and coordination shifts (in parentheses), alongside multiplicities and coupling constants (J_{C-H}), for the ligands **L1–L4** and the corresponding gold(III) complexes **1–4** in CDCl₃.

	L1 ^a	[AuCl ₃ (L1)] (1) ^b	L2 ^a	[AuCl ₃ (L2)] (2) ^c	L3	[AuCl ₃ (L3)] (3)	L4	[AuCl ₃ (L4)] (4)
C-1	53.7	55.3, m (+1.6)	53.7	55.3, m (+1.6)	53.8, bs	56.2, m (+2.4)	53.6, bs	58.6, bs (+5.0)
C-2	31.9	31.4, pt, $J = 135.4$ Hz ^d (−0.5)	31.9	31.4, pt, $J = 135.4$ Hz (−0.5)	31.9, ptquin, $J = 134.4, 5.8, 3.6$ Hz	31.4, m, ^e $J_{1,2} = 136.3$ Hz (−0.5)	31.9, ptquin, $J = 133.8, 4.1$ Hz	31.8, bpt, $J = 134.1$ Hz (−0.1)
C-3	24.7	23.7, bt, $J = 136.3$ Hz (−1.0)	24.7	23.7, bt, $J = 136.3$ Hz (−1.0)	24.7, ptt, $J = 134.6, 2.8$ Hz	23.7, bpdd, $J = 138.3, 135.7$ Hz (−1.0)	24.8, pddt, $J = 136.4, 130.8, 3.2$ Hz	24.4, bpt, $J = 134.9$ Hz (−0.4)
C-4	53.3	56.5, m, $J = 149.4$ Hz (+3.2)	53.2	56.3, m, ^e $J_{1,2} = 149.4$ Hz (+3.1)	53.2, bd, $J = 146.8$ Hz	56.4, m, ^e $J_{1,2} = 151.7$ Hz (+3.2)	53.4, bd, $J = 147.6$ Hz	53.7, bpd, $J = 138.8$ Hz (+0.3)
C-4a	163.7	164.1, m (+0.4)	162.9	163.4, m (+0.5)	163.1, bs	163.8, m (+0.7)	162.6, m	165.6, m (+3.0)
C-5a	141.5	135.0, d, $J = 7.4$ Hz (−6.5)	139.8	133.2, m ^f (−6.6)	141.2, d, $J = 8.8$ Hz	135.1, d, $J = 9.7$ Hz (−6.1)	140.4, bs	143.1, bs (+2.7)
C-6	128.1	124.2, pdquin, $J = 161.1, 5.5$ Hz (−3.9)	128.0	124.7, d, $J = 163.4$ Hz (−3.3)	126.4, dd, $J = 161.3, 7.3$ Hz	123.0, dd, $J = 164.1, 8.1$ Hz (−3.4)	136.7, pquin, $J = 6.4$ Hz	138.8, pquin, $J = 6.7$ Hz (+2.1)
C-7	138.3	143.1, m (+4.8)	129.9	133.3, m ^g (+3.4)	127.6, d, $J = 159.7$ Hz	131.0, d, $J = 164.4$ Hz (+2.4)	128.5, ddq, $J = 158.4, 10.6, 5.2$ Hz	131.9, ddq, $J = 162.0, 8.1, 5.4$ Hz (+3.4)
C-8	129.9	133.4, ddq, $J = 161.4, 7.4, 5.0$ Hz (+3.5)	138.3	142.5, m (+4.2)	128.4, ddq, $J = 158.2, 9.3, 4.9$ Hz	131.7, ddq, $J = 161.7, 8.2, 4.8$ Hz (+3.3)	127.5, d, $J = 159.9$ Hz	131.1, d, $J = 164.6$ Hz (+3.6)
C-9	128.3	129.5, d, $J = 165.8$ Hz (+1.2)	128.2	129.1, m, $J = 165.2$ Hz (+0.9)	137.3, pquin, $J = 5.9$ Hz	139.1, pquin, $J = 7.0$ Hz (+1.8)	126.8, dd, $J = 161.8, 7.4$ Hz	124.3, dd, $J = 163.6, 8.1$ Hz (−2.5)
C-9a	139.5	143.2, m (+3.7)	141.3	144.5, m (+3.2)	140.5, m	143.5, m (+3.0)	141.5, d, $J = 8.9$ Hz	136.0, d, $J = 10.5$ Hz (−5.5)
C-10a	164.6	167.4, m (+2.8)	165.4	168.4, m (+3.0)	164.1, bs	167.0, m (+2.9)	164.8, m	164.7, m (−0.1)
C-11	54.2	56.2, m (+2.0)	54.2	56.1, m (+1.9)	54.2, bs	55.4, m (+1.2)	54.2, bs	55.8, m (+1.6)
C-1'	10.1	10.2, qd, $J = 127.4, 2.4$ Hz (+0.1)	10.0	10.2, qd, $J = 127.4, 2.4$ Hz (+0.2)	10.0, qd, $J = 126.1, 2.5$ Hz	10.1, qd, $J = 127.2, 2.4$ Hz (+0.1)	10.0, qd, $J = 126.1, 2.5$ Hz	13.3, qd, $J = 127.3, 2.7$ Hz (+3.3)
C-7'/8'/9'/6'	21.6	22.1, qd, $J = 128.0, 4.3$ Hz (+0.5)	21.5	21.6, qd, $J = 128.5, 4.1$ Hz (+0.1)	17.2, qd, $J = 127.8, 4.5$ Hz	17.7, qd, $J = 128.8, 4.8$ Hz (+0.5)	17.7, qd, $J = 127.6, 4.8$ Hz	17.9, qd, $J = 128.7, 4.8$ Hz (+0.2)
C-11' (syn)	20.3	20.7, qq, $J = 126.1, 4.7$ Hz (+0.4)	20.3	20.7, qq, $J = 126.1, 4.7$ Hz (+0.4)	20.3, qq, $J = 125.4, 4.9$ Hz	20.8, qq, $J = 126.4, 4.8$ Hz (+0.5)	20.3, qq, $J = 126.3, 5.5$ Hz	20.9, qq, $J = 126.2, 4.9$ Hz (+0.6)
C-11'' (anti)	18.5	18.8, qq, $J = 126.4, 4.2$ Hz (+0.3)	18.5	18.8, qq, $J = 126.4, 4.2$ Hz (+0.3)	18.6, qq, $J = 125.2, 4.6$ Hz	18.2, qq, $J = 126.0, 4.5$ Hz (−0.4)	18.6, qq, $J = 125.7, 5.0$ Hz	18.5, qq, $J = 125.6, 4.8$ Hz (−0.1)

^a **L1** and **L2** chemical shifts and coupling constants were determined by 1D/2D NMR analyses of mixture of ligands **L1** and **L2**.

^b The results of the NMR analyses of pure [AuCl₃(**L1**)], which was isolated by fractional crystallization of [AuCl₃(**L1**)]/[AuCl₃(**L2**)] mixture from deuterated chloroform.

^c [AuCl₃(**L2**)] chemical shifts and coupling constants were determined by 1D/2D NMR analyses of [AuCl₃(**L1**)]/[AuCl₃(**L2**)] mixture.

^d J_{C-H} coupling constants (chemical shifts were retrieved from ¹³C{¹H} NMR analysis; J_{C-H} were retrieved from proton–carbon coupled NMR experiments).

^e A complex doublet of multiplets.

^f Partially overlapped with **L1** C-8 and **L2** C-7.

^g Overlapped with **L1** C-8 and **L2** C-5a; bd-broad doublet, bpdd-broad pseudo doublet of doublets, bs-broad singlet, bt-broad triplet, d-doublet, dd-doublet of doublets, ddq-doublet of doublet of quartets, bpd-broad pseudo doublet, bpt-broad pseudo triplet, m-multiplet, pddt-pseudo doublet of doublet of triplets, pdquin-pseudo doublet of quintets, pt-pseudo triplet, ptt-pseudo triplet of triplets, ptquin-pseudo triplet of quintets, pquin-pseudo quintet, qd-quartet of doublets, qq-quartet of quartets.

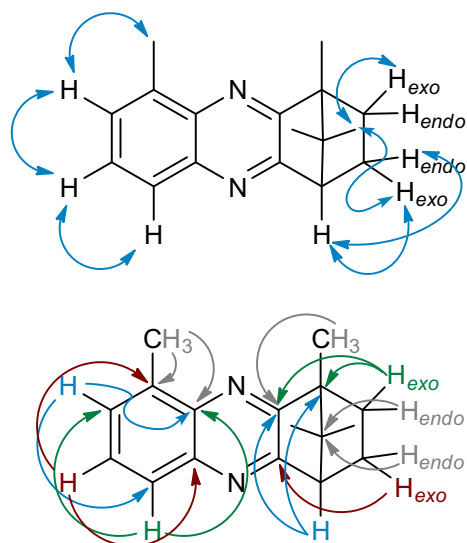


Fig. 3. Key experimentally observed NOESY (top) and HMBC (bottom) interactions (marked with arrows) of ligand **L4**; analogous correlations were found for other ligands and all complexes; for clarity, HMBC correlations are given as arrows of different colors (these match the color of the corresponding H-atoms: blue – H-4 and H-8, green – H-2*exo* and H-6, red – H-3*exo* and H-7, gray – H-2*endo*, H-3*endo* and H-9); all HMBC interactions of all studied compounds are summarized in Table S2. (Color online.)

respectively); $J_{AB} = 9.5$ Hz, $J_{AH} = 4.3$ Hz, $J_{AM} = -13.5$ Hz, $J_{AX} = 1.4$ Hz, $J_{BH} = -13.2$ Hz, $J_{BM} = 4.4$ Hz, $J_{BX} = -0.1$ Hz, $J_{HM} = 11.1$ Hz, $J_{HX} = -0.3$ Hz, $J_{MX} = 4.5$ Hz, while for **L4** δ H (ppm) were 2.290, 2.045, 1.408 and 1.402 (for H-3*exo* (M), H-2*exo* (H), H-3*endo* (B), H-2*endo* (A), respectively); $J_{AB} = 9.3$ Hz, $J_{AH} = -13.8$ Hz, $J_{AM} = 4.4$ Hz, $J_{AX} = -0.1$ Hz, $J_{BH} = 4.3$ Hz, $J_{BM} = -13.2$ Hz, $J_{BX} = 0.6$ Hz, $J_{HM} = 11.2$ Hz, $J_{HX} = -0.2$ Hz, $J_{MX} = 4.4$ Hz. The values of the coupling constants determined by using WINDNMR simulation are in excellent agreement with the optimized geometries of **L1–L4**, e.g. J values for the synperiplanar protons were 9.3–11.2 Hz, and those of synclinal were around 4.3 Hz (Figs. S1, S3 and S4).

It is interesting to note that although the synthesis of 8-methylcamphorquinoxaline was already previously reported [54], it seems that, according to the spectral data given in that paper, the claimed condensation of camphorquinone and 4-methyl-1,2-benzenediamine was in fact unsuccessful. The reported NMR chemical shifts correspond to a mixture of the unchanged reagents and not to the target compound and are not in agreement even with the spectral data of similar compounds from the very same paper.

Only one family of proton/carbon signals was observed in the CDCl₃ solutions of **1–4**. This means that either one complex for each of the studied ligands was present in CDCl₃ solution or that a fast (on the NMR time scale) equilibrium between two possible regioisomeric complexes exists. The position of Au(III) coordination (bonding to which of the two different nitrogen atoms, N-5 or N-10) was deduced from the (largest) values of the observed $\Delta(^1\text{H})_{\text{coord}}$ coordination shifts (determined in respect to the free

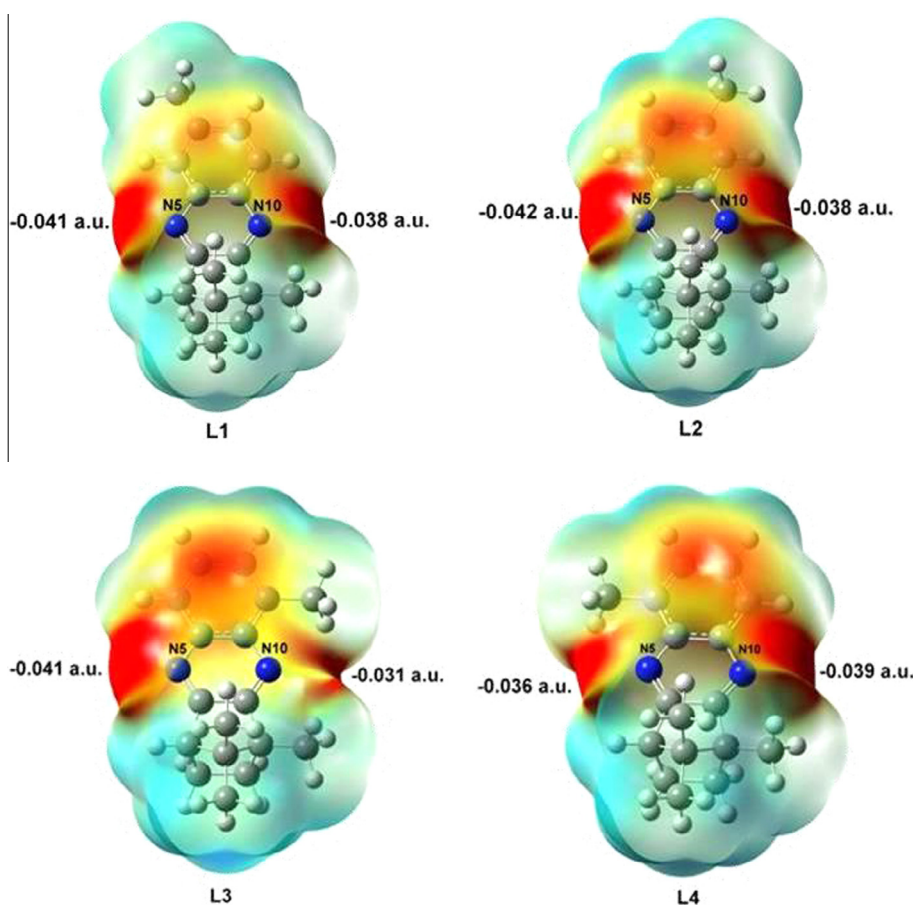


Fig. 4. Electrostatic potential mapped on electron density surfaces for the investigated methylcamphorquinoxaline ligands **L1–L4** generated at DFT M06-2X/cc-PVTZ//M06-2X/cc-PVDZ level of theory (isoval 0.0004 a.u.). Color change from red most negative to blue most positive. (Color online.)

L1–L4 in CDCl_3) in the ^1H NMR spectra of **1–4**. These coordination shifts for **1–4** are summarized in Table 3, and are, for clarity, given in parallel in Figs. S5 and S6.

$\Delta(^1\text{H})_{\text{coord}}$ values confirmed that **L1–L3** coordinated to Au(III) via the less sterically hindered nitrogen atom N-5: $\Delta(^1\text{H})_{\text{coord}}$ was the highest for H-4 (c.a. 0.8 ppm; the coordination shift for, H-1', was significantly lower – c.a. 0.1), followed by that for H-6 (c.a. 0.6 ppm; the coordination shift for its counterpart, H-9, was significantly lower – c.a. 0.2). Contrary to that, in the case of **L4**, which coordinated the AuCl_3 moiety via N-10, the highest $\Delta(^1\text{H})_{\text{coord}}$ was observed for H-9 and H-1' (c.a. 0.8 ppm; the coordination shifts for, H-6' and H-4, were significantly lower – less than 0.1 and 0.25, respectively). Almost identical coordination shifts for the equivalent protons in the spectra of **1–4** (Fig. S5; in the case of **4**, due to the coordination via N-10 instead of N-5 atom, these are inverse to that of **1–3**) excluded the possibility of a fast equilibrium between regioisomeric complexes of a single ligand. In the case of such equilibrium, the resulting NMR spectra would be an average between the spectra of the pure regioisomeric complexes of a single ligand (N-5 and N-10 coordination) that takes into account their respective molar ratios in solution. Having in mind the results of the theoretical study (*vide infra*), it is not likely that these molar ratios would be identical for **1–3**, and inverse for **4**. The differences in the distribution of the mentioned coordination products of a single ligand should result in significantly different values of the coordination shifts for **L1–L4**, which was not the case (Table 3; Figs. S5 and S6).

As can be seen from Table 3 and Fig. S5, all ^1H NMR signals were shifted downfield and by an almost identical mean δ value ($\Delta_{\text{H}}(\mathbf{1}) = +0.26$, $\Delta_{\text{H}}(\mathbf{2}) = +0.26$, $\Delta_{\text{H}}(\mathbf{3}) = +0.29$ and $\Delta_{\text{H}}(\mathbf{4}) = +0.30$ ppm for all complexes; all protons were taken into account). Equivalent average coordination shifts for Au(III) complexes of the previously studied diazine ligands (including quinoxaline) was c.a. twofold higher ($\Delta_{\text{H}}: +0.59\text{--}0.64$ ppm) [25,26].

Qualitatively, the downfield shifts which occurred for the protons in the mentioned complexes were ascribed to a delocalization of the charge deficiency (formation of formal cation (N^+) by gold (III) coordination) throughout the rings of the diazine heteroaromatic ligands [26]. In the case of the polycyclic ligands (quinoxaline and phenazine), the charge deficiency was distributed more or less uniformly through the benzocyclic rings in the corresponding complexes. This, however, seems not to be the case in **1–4** (Fig. S5).

Although on the whole, Au(III) complexation of the ligands produced an overall deshielding of ring carbons (mean $\Delta_{\text{C}}(\mathbf{1}) = +0.7$, $\Delta_{\text{C}}(\mathbf{2}) = +0.7$, $\Delta_{\text{C}}(\mathbf{3}) = +0.6$ and $\Delta_{\text{C}}(\mathbf{4}) = +1.0$ ppm), in complexes **1–4**, the signals of several carbon atoms were shifted upfield ($\Delta(^{13}\text{C})_{\text{coord}}$ coordination shifts for **1–4** are given in Table 4 and Fig. S6). This effect was most pronounced in the case of C-6 and C-5a in **1–3** and C-9 and C-9a in **4**. These were shifted upfield by -2.5 to -3.9 (C-6/C-9), and by -5.5 to -6.6 ppm (C-5a/C-9a) (Fig. S6). This is in accordance with the coordination shifts observed for quinoxaline (qx) and phenazine (phz) complexes of Au(III) [25], but is not in agreement with the shielding/deshielding pattern for the other diazine complexes of Au(III) [26].

3.4. Theoretical studies

In order to gain a better understanding of the coordination mode of **L1–L4** toward the AuCl_3 fragment, we optimized their structures (Fig. S2) and examined their molecular electrostatic potential (MEP) mapped on electron density surface generated at M06-2X/cc-PVTZ//M06-2X/cc-PVDZ level of theory (Fig. 4). The MEP has been shown so far as a very useful in prediction of the sites of electrophilic and nucleophilic attack, as well as hydrogen bonding interactions [55,56]. The regions of negative potentials

colored in red are related to the possible sites of electrophilic attack, while the regions of positive potential (blue) may indicate the sites of nucleophilic attack. As can be expected, the negative potential sites for methylcamphorquinoxaline ligands **L1–L4** are on the electronegative nitrogen atoms N5 and N10. However, from

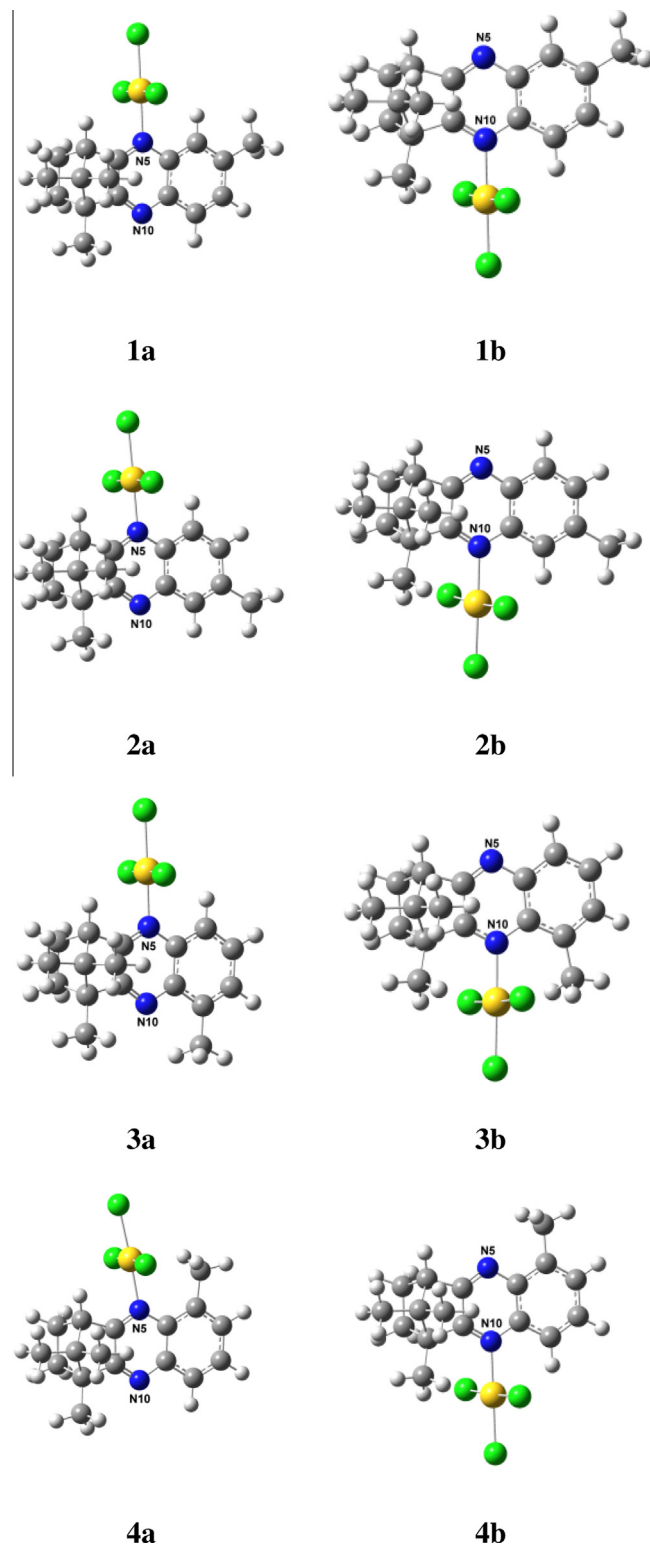


Fig. 5. The structures of eight mononuclear gold(III) complexes with the methylcamphorquinoxaline ligands **L1–L4** (**1a–4a** for N-5 and **1b–4b** for N-10 binding site) calculated at DFT M06-2X/(LanL2TZ(f)+cc-PVTZ)//M06-2X/(LanL2TZ(f)+cc-PVDZ) level of theory.

the values of the negative electrostatic potentials on these two nitrogens, it can be concluded that N5 atom is a more favorable site for an Au(III) electrophilic attack in **L1–L3**, while only in the case of **L4**, the N10 is the more favorable one (Fig. 4).

The calculations have been then extended to the gold(III) complexes with the methylcamphorquinoxaline ligands **L1–L4**. Due to the presence of two potential metal-binding nitrogen atoms in the ligands, two possible interaction schemes for an Au(III) metal center were subjected to computational studies, gold(III) complexes in which the corresponding ligand is coordinated through N-5 (**1a–4a**) and N-10 nitrogen atom (**1b–4b**) (Fig. 5). It is important to note that complexes **1a–3a** and **4b** were isolated as the products of the reactions between methylcamphorquinoxaline ligands **L1–L4** and $[\text{AuCl}_4]^-$ and characterized by NMR and X-ray methods (*vide supra*, complexes **1–4**). Upon comparison of the three different theoretical approaches (see Experimental part), the M06-2X functional [35] was chosen to optimize structures and to calculate energies both in the gas phase and solution. This functional, in terms of Au–N and Au–Cl bonds lengths, as well as the corresponding angles around Au(III) ion, showed the best agreement with the respective crystal structures of **1–4**. The structures of the eight mononuclear gold(III) complexes calculated at M06-2X/(LanL2TZ(f)+cc-PVTZ)//M06-2X/(LanL2TZ(f)+cc-PVDZ) level of theory are displayed in Fig. 5, while their relative energies both in the gas phase and ethanol are presented in Table 5. As can be seen from this table, complexes **1b–3b** in which the Au(III) ion is bound to the N-10 nitrogen of **L1–L3**, respectively, were calculated to be higher in energy than **1a–3a**, suggesting that the energetically preferred structure has the corresponding ligand attached to the Au(III) center via the N-5 nitrogen atom. These differences, albeit small, well mirror the experimentally observed selectivity in the corresponding complexation reactions. Moreover, the differences in energy are greater in ethanol, which means that the use of this solvent additionally aides the formation of **1a–3a**. On the other hand, energy of **4a** is higher than that of **4b** indicating that N-10 coordination mode of **L4** is energetically favorable (Table 5). These theoretical findings are in line with our NMR and X-ray results, all together supporting the very selective formation of gold(III) complexes in which, generally speaking, the corresponding methylcamphorquinoxaline ligand was coordinated via the less sterically hindered nitrogen.

Table 5

Relative energies (kcal/mol) of eight gold(III) complexes with the methylcamphorquinoxaline ligands **L1–L4** both in the gas phase and ethanol obtained in M06-2X calculations using a composite basis set.

Ligand	Gold(III) complex	Relative energy (kcal/mol)	
		In vacuum M06-2X/Gen	In ethanol M06-2X/Gen
L1	1a	0.0 ^a	0.0 ^e
	1b	1.0	1.6
L2	2a	0.0 ^b	0.0 ^f
	2b	0.8	1.7
L3	3a	0.0 ^c	0.0 ^g
	3b	5.5	7.8
L4	4a	2.1	2.7 ^h
	4b	0.0 ^d	0.0

Absolute energy baselines (in hartree).

^a 2285.327136.

^b 2285.326867.

^c 2285.327084.

^d 2285.325861.

^e 2285.346237.

^f 2285.346291.

^g 2285.346427.

^h 2285.343533.

4. Conclusions

We have demonstrated that chiral methylcamphorquinoxaline ligands **L1–L4** can selectively bind to Au(III) to form discrete mononuclear complexes, in which they act as monodentate ligands, regardless of stoichiometric ratio of the reactants. Ligands **L1–L3** coordinate to Au(III) through the less hindered (N-5) of the two nonequivalent nitrogen atoms (N-5 and N-10). However, placing of the methyl substituent in a direct neighborhood of N-5 resulted in inversion of the ligating properties of the two nitrogen atoms. This has been explained by bigger steric hindrance exerted by the methyl group attached to the aromatic ring than the methyl group attached to the Csp^3 carbon. Moreover, it has been shown that upon auration the methylcamphorquinoxaline ligands **L1** and **L2** that co-eluted in a number of mobile phases, form stable complexes that can be separated by fractional crystallization.

Acknowledgements

This work was funded in part by the Ministry of Education, Science and Technological Development of the Republic of Serbia (Projects No. 172036 and 172061) and was also supported by the Polish Grid Infrastructure PL-Grid. B.Đ.G. gratefully acknowledges the financial support from the Ministry of Education, Science and Technological Development of the Republic of Serbia during her postdoctoral stay at the Adam Mickiewicz University, Poznań, Poland.

Appendix A. Supplementary data

CCDC 1413257–1413260 contains the supplementary crystallographic data for **1–4**. These data can be obtained free of charge via <http://www.ccdc.cam.ac.uk/conts/retrieving.html>, or from the Cambridge Crystallographic Data Centre, 12 Union Road, Cambridge CB2 1EZ, UK; fax: (+44) 1223-336-033; or e-mail: deposit@ccdc.cam.ac.uk. Supplementary data associated with this article can be found, in the online version, at <http://dx.doi.org/10.1016/j.poly.2015.12.009>.

References

- [1] C.J. Sumbly, *Coord. Chem. Rev.* 255 (2011) 1937.
- [2] C. Kaes, A. Katz, M.W. Hosseini, *Chem. Rev.* 100 (2000) 3553.
- [3] P.J. Steel, *Coord. Chem. Rev.* 106 (1990) 227.
- [4] C.J. Sumbly, (Ph. D. Thesis), University of Canterbury, Christchurch, New Zealand, 2003.
- [5] D.P. Ašanin, M.D. Živković, S. Rajković, B. Waržajtis, U. Rychlewska, M.I. Djuran, *Polyhedron* 51 (2013) 255.
- [6] E.G. Brown, *Ring Nitrogen and Key Biomolecules: The Biochemistry of N-Heterocycles*, Kluwer Academic Publishers, The Netherlands, 1998.
- [7] P.J. Steel, *Molecules* 9 (2004) 440.
- [8] S. Derossi, M. Casanova, E. Iengo, E. Zangrando, M. Stener, E. Alessio, *Inorg. Chem.* 46 (2007) 11243.
- [9] M. Willermann, C. Mulcahy, R.K.O. Sigel, M.M. Cerdà, E. Freisinger, P.J. Sanz Miguel, M. Roitzsch, B. Lippert, *Inorg. Chem.* 45 (2006) 2093.
- [10] S. Rajković, U. Rychlewska, B. Waržajtis, D.P. Ašanin, M.D. Živković, M.I. Djuran, *Polyhedron* 67 (2014) 279.
- [11] V. Balzani, A. Juris, M. Venturi, S. Campagna, S. Serroni, *Chem. Rev.* 96 (1996) 759.
- [12] D.E. Fenton, *Chem. Soc. Rev.* 28 (1999) 159.
- [13] A.M. Barrios, S.J. Lippard, *Inorg. Chem.* 40 (2001) 1250.
- [14] A.M. Barrios, S.J. Lippard, *Inorg. Chem.* 40 (2001) 1060.
- [15] A.K. Parhi, Y. Zhang, K.W. Saionz, P. Pradhan, M. Kaul, K. Trivedi, D.S. Pilch, E.J. LaVoie, *Bioorg. Med. Chem. Lett.* 23 (2013) 4968.
- [16] H. Ishikawa, T. Sugiyama, K. Kurita, A. Yokoyama, *Bioorg. Chem.* 41–42 (2012) 1.
- [17] F.A.R. Rodrigues, I.da S. Bomfim, B.C. Cavalcanti, C.do Ó. Pessoa, J.L. Wardell, S. M.S.V. Wardell, A.C. Pinheiro, C.R. Kaiser, T.C.M. Nogueira, J.N. Low, L.R. Gomes, M.V.N. de Souza, *Bioorg. Med. Chem. Lett.* 24 (2014) 934.
- [18] L.E. Seitz, W.J. Suling, R.C. Reynolds, *J. Med. Chem.* 45 (2002) 5604.
- [19] J. Guillon, I. Forfar, M. Mamani-Matsuda, V. Desplat, M. Saliège, D. Thiolat, S. Massip, A. Tabourier, J.-M. Léger, B. Dufaure, G. Haumont, C. Jarry, D. Mossalayi, *Bioorg. Med. Chem.* 15 (2007) 194.

- [20] J. Guillon, S. Moreau, E. Mouray, V. Sinou, I. Forfar, S.B. Fabre, V. Desplat, P. Millet, D. Parzy, C. Jarry, P. Grellier, *Bioorg. Med. Chem.* 16 (2008) 9133.
- [21] R. Sarges, H.R. Howard, R.G. Browne, L.A. Lebel, P.A. Seymour, B.K. Koe, *J. Med. Chem.* 33 (1990) 2240.
- [22] C. Srinivas, C.N.S. Sai Pavan Kumar, V. Jayathirtha Rao, S. Palaniappan, *Catal. Lett.* 121 (2008) 291.
- [23] B. Bertrand, A. Casini, *Dalton Trans.* 43 (2014) 4209.
- [24] B.Đ. Glišić, M.I. Djuran, *Dalton Trans.* 43 (2014) 5950.
- [25] B.Đ. Glišić, B. Warzajtis, N.S. Radulović, U. Rychlewska, M.I. Djuran, *Polyhedron* 87 (2015) 208.
- [26] B. Warzajtis, B.Đ. Glišić, N.S. Radulović, U. Rychlewska, M.I. Djuran, *Polyhedron* 79 (2014) 221.
- [27] J.C. Howard, *Org. Synth.* 35 (1955) 3.
- [28] A.I. Vogel, *Vogel's Textbook of Practical Organic Chemistry*, 5th ed., Longman Scientific and Technical, Harlow, 1989.
- [29] J.D. White, D.J. Wardrop, K.F. Sundermann, *Org. Synth.* 79 (2002) 125.
- [30] C.M. Fitchett, P.J. Steel, *Arkivoc* 2006 (2006) 218.
- [31] CrysAlis PRO, Agilent Technologies, Yarnton, Oxfordshire, England, 2013.
- [32] R.C. Clark, J.S. Reid, *Acta Crystallogr., Sect. A* 51 (1995) 887.
- [33] G.M. Sheldrick, *Acta Crystallogr., Sect. A* 64 (2008) 112.
- [34] I.J. Bruno, J.C. Cole, P.R. Edgington, M. Kessler, C.F. Macrae, P. McCabe, J. Pearson, R. Taylor, *Acta Crystallogr., Sect. B* 58 (2002) 389.
- [35] Y. Zhao, D.G. Truhlar, *J. Chem. Phys.* 125 (2006) 194101.
- [36] A.D. Becke, *J. Chem. Phys.* 98 (1993) 5648.
- [37] C. Lee, W. Yang, R.G. Parr, *Phys. Rev. B* 37 (1988) 785.
- [38] S. Niu, M.B. Hall, *Chem. Rev.* 100 (2000) 353.
- [39] A.P. Martins, A. Marrone, A. Ciancetta, A.G. Cobo, M. Echevarría, T.F. Moura, N. Re, A. Casini, G. Soveral, *PLoS One* 7 (2012) e37435.
- [40] Y. Zhao, D.G. Truhlar, *Chem. Phys. Lett.* 502 (2011) 1.
- [41] R.G.A.R. MacLagan, S. Gronert, M. Meot-Ner, *J. Phys. Chem. A* 119 (2015) 127.
- [42] T.H. Dunning Jr., *J. Chem. Phys.* 90 (1989) 1007.
- [43] D.E. Woon, T.H. Dunning Jr., *J. Chem. Phys.* 98 (1993) 1358.
- [44] P.J. Hay, W.R. Wadt, *J. Chem. Phys.* 82 (1985) 270.
- [45] J. Tomasi, B. Mennucci, R. Cammi, *Chem. Rev.* 105 (2005) 2999.
- [46] J.R. Cheeseman, G.W. Trucks, T.A. Keith, M.J. Frisch, *J. Chem. Phys.* 104 (1996) 5497.
- [47] H.F. Schaefer III, *Modern Theoretical Chemistry*, vol. 3, Plenum, New York, 1976.
- [48] A.E. Reed, L.A. Curtiss, F. Weinhold, *Chem. Rev.* 88 (1988) 899.
- [49] M.J. Frisch et al., *GAUSSIAN 09*, Revision D.01, Gaussian Inc., Wallingford CT, 2013.
- [50] Y.-W. Li, Y. Tao, L.-F. Wang, T.-L. Hu, X.-H. Bu, *RSC Adv.* 2 (2012) 4348.
- [51] C.M. Fitchett, P.J. Steel, *Aust. J. Chem.* 59 (2006) 19.
- [52] J.G. Napolitano, D.C. Lankin, T.N. Graf, J.B. Friesen, S.-N. Chen, J.B. McAlpine, N. H. Oberlies, G.F. Pauli, *J. Org. Chem.* 78 (2013) 2827.
- [53] H.J. Reich, *J. Chem. Educ.* 72 (1995) 1086.
- [54] M.J. Hosseini-Sarvari, *Iran Chem. Soc.* 9 (2012) 535.
- [55] F.J. Luque, J.M. López, M. Orozco, *Theor. Chem. Acc.* 103 (2000) 343.
- [56] R.V. Pinjari, S.P. Gejji, *J. Phys. Chem. A* 112 (2008) 12679.